JOURNAL OF AGRICULTURAL AND FOOD CHEMISTRY

ARTICLE

pubs.acs.org/JAFC

Pterocarpan Profiles for Soybean Leaves at Different Growth Stages and Investigation of Their Glycosidase Inhibitions

Heung Joo Yuk,[†] Marcus J. Curtis-Long,[§] Hyung Won Ryu,[†] Ki Chang Jang,[⊥] Woo Duck Seo,[⊥] Jun Young Kim,[⊥] Kyu Young Kang,[†] and Ki Hun Park*[,†]

[†]Division of Applied Life Science (BK21 Program), IALS, Graduate School of Gyeongsang National University, Jinju 660-701, Republic of Korea

[§]Graduate Program in Biochemistry and Biophysics, Brandeis University, 415 South Street, Woltham, Massachusetts 02453, United States

[⊥]Department of Functional Crop, NICS, RDA, Miryang 627-803, Republic of Korea

ABSTRACT: Soybean leaves are eaten as seasonal edible greens in Korea. Analysis of the ethyl acetate extract of these leaves showed that it exhibited potent and selective neuraminidase inhibition, which began at the R3 stage and peaked at R7. Ten pterocarpans, including the new 6a-hydroxypterocarpan **10**, were isolated from soybean leaves and their inhibition activities tested against a range of glycosidases. The relationship between structure and enzyme inhibition was investigated: 6a-hydroxypterocarpans exhibited much higher inhibition against neuraminidase (IC_{50} = 2.4−89.4 μM) than α-glucosidase (IC_{50} = 90.4− >100 μM). Glyceollin VII (**7**) displayed 40-fold greater activity (IC_{50} = 2.4 μM) against neuraminidase than α-glucosidase (IC_{50} = 90.4 μM). On the other hand, coumestanes (**1**−**3**) were good α-glucosidase inhibitors (IC_{50} = 6.0−42.6 μM). In kinetic analysis, the most potent neuraminidase inhibitors (**5**−**10**) were noncompetitive. HPLC analysis indicated that most pterocarpan synthesis began from the R3 stage, and a rapid change of pterocarpan concentrations was observed between the R4 and R7 stages.

KEYWORDS: glycosidase, neuraminidase, soy leaf, pterocarpans, glyceollin

INTRODUCTION

Glycosylation is one of the key modifications of proteins. It can affect protein stability, localization, and cell signaling.[1,2] It is thus of no surprise that the study of glycosidase inhibition has been pursued vigorously. Two important glycosidases are α-glucosidase and neuraminidase, which respectively remove terminal glucose or sialic acids from glycans. Inhibition of α-glucosidase has a profound effect on glycan structure, which consequently affects the protein maturation, transport, secretion, and cell−cell or cell−virus recognition processes.[3,4] It also has interest in diabetes research because it can also retard the cleavage of complex carbohydrates and attenuate postprandial glucose absorption, thus regulating blood sugar levels. Neuraminidase specifically cleaves *N*-acetylneuraminic acid (Neu5Ac) from cell-surface glycoproteins when sialic acids are joined to galactose via an α2→3 or α2→6 linkage.[5,6] Neuraminidase plays immensely important roles in biological recognition by virtue of being situated at the outer periphery of the cell surface, where it participates in numerous interactions that a cell makes with its microenvironment. Thus, neuraminidase inhibitors can contribute to the control of cancer development, viral/bacterial infection, and inflammatory response.[7,8]

In recent years, many papers have reported that pterocarpans constitute a basis for significant α-glucosidase and neuraminidase inhibitions.[9] Pterocarpans are found almost exclusively in the Leguminosae or Fabaceae plant families, because they are formed by an unusual ring cyclization of isoflavones, which occurs only in these species. Soybean is considered to be one of the richest sources of isoflavones, including pterocarpans, which are representative phytoalexins that plants use to kill pathogens.[10] Pterocarpans are also well-known polyphenols with antioxidant properties.[11] They also display estrogenic activity that can prevent osteoporosis and breast and prostate cancer.[12] Thus, an array of biological properties remain to be found in the study and isolation of pterocarpans, and with this in mind we set about this work. We are particularly interested in correlating properties of the crude leaf extract, where the majority of secondary metabolites exist, having isolated and characterized biochemically the compounds. Because soybean leaves have long been used as seasonal edible greens in Korea, these data are directly relevant to the food industry. In this study, we show that ethyl acetate extracts of soybean leaves display potent and selective inhibition of neuraminidase and α-glucosidase activities. This inhibition emerges across the development stages of the plant, becoming most significant in the R7 phase. In all, 10 glycosidase inhibitory pterocarpans (**1**−**10**) were isolated, including new pterocarpan **10**. These were the most prevalent in the plant at the R7 phase.

MATERIALS AND METHODS

General Apparatus and Chemicals. Melting points were measured on a Thomas Scientific capillary apparatus. CD spectra were

Received: August 18, 2011
Revised: October 7, 2011
Accepted: October 11, 2011
Published: October 11, 2011

Table 1. ^{1}H and ^{13}C NMR Data of New Compound 10 in CD_3OD[a]

position	δ_H (J in Hz)	δ_C	HMBC
1		161.3	
2		118.8	
3		161.5	
4	6.30 (1H, s)	97.3	C-2,3,4a,11a,b
4a		156.6	
6	(6α) 3.86 (1H, d, J = 11.3 Hz); (6β) 4.05 (1H, d, J = 11.3 Hz)	71.4	C-4a,6b,11a
6a		77.3	
6b		121.7	
7	7.15 (1H, d, J = 8.1 Hz)	125.4	C-6a,8,9,10a
8	6.40 (1H, d, J = 8.1 Hz)	109.7	C-6b,9,10
9		161.7	
10	6.25 (1H, s)	99.4	C-6b,8,9
10a		162.5	
11a	5.33 (1H, s)	83.3	C-1,4a,6,6a,6b,11b
11b		108.5	
1′	3.27 (2H, m)	24.1	C-1, 2,3,2′,3′
2′	5.15 (1H, m)	125.2	C-1′,4′,5′
3′		132.1	
4′	1.75 (3H, s)	18.4	C-2′,3′,5′
5′	1.67 (3H, s)	26.3	C-2′,3′,4′
3-OCH_3	3.90 (3H, s)	63.8	C-3
9-OCH_3	3.75 (3H, s)	56.5	C-9

[a] Assignments were made by ^{1}H−^{1}H COSY, HMQC and HMBC data.

recorded on a JASCO J-715 spectropolarimeter, and optical rotations were measured on a Perkin-Elmer 343 polarimeter. NMR spectra were recorded on a Bruker AM 500 spectrometer with TMS as an internal standard, and chemical shifts are expressed in δ values. EIMS and HREIMS were obtained on a JEOL JMS-700 mass spectrometer (JEOL, Tokyo, Japan). Qualitative analyses were made using a Perkin-Elmer HPLC S200 (Perkin-Elmer, Bridgeport, CT). All purifications were monitored on commercially available glass-backed Merck precoated TLC plates and visualized under UV at 254 and 366 nm or stained with 10% H_2SO_4 solution. Silica gel (230−400 mesh, Merck), RP-18 (ODS-A, 12 nm, S-150 μM, YMC), and Sephadex LH-20 (Pharmacia Biotech AB, Uppsala, Sweden) were used for column chromatography. All solvents used for extraction and isolation were of analytical grade.

Plant Material and Extraction. Soybeans, *Glycine max* (L.) Merrill, were cultivated at Jinju in the experimental field of Gyeongsang National University, Gyeongsangnam-do, Korea. The leaves of soybean were collected over a period of 3 months (R1 stage, July 12, to R7 stage, September 27, 2009). The collected leaves were freeze-dried immediately after sampling and stored at −40 °C until needed. Prior to further analysis, leaves were thawed and cut into small pieces with a laboratory blade cutter. All sample masses were based on dry weight. Two grams of chopped leaves was extracted (with shaking) into 20 mL of ethyl acetate at room temperature for 24 h. Suitable filtered aliquots were then used for enzymatic assays and HPLC analyses. Soybean leaves were harvested from each replicate plant at different stages as follows. The R3 and R4 stages are the beginning period of pod growth and the period of full pod, respectively. The R5 stage is the beginning period during which the seed length increases rapidly and the pods fill. At this point, nutrients are being redistributed from the plant to the seeds, which are approximately 3 mm long. The R6 stage is the period when the pods fill with fully grown green seeds and the leaves gradually turn yellow. The R7 stage is physiological maturity, when the seeds become brown and the plant continues to lose leaves and dry down.

HPLC Analysis. Quantification of the relative abundance of the compounds isolated and assayed in this paper within the crude leaf extract was carried out by HPLC (Perkin-Elmer 200 series) using a Zorbax SB-C 18 column (4.6 × 150 mm, 5 μM, Agilent, Santa Clara, CA). Absorbances were measured at 280 nm. About 10 μL of crude leaf extract was loaded onto the column. Gradient elution was carried out with water/0.1% acetic acid (solvent A) and acetonitrile (solvent B) at a constant flow rate of 1.0 mL/min. The linear gradient elution program was as follows: 0−5 min, 5−45% B; 5−10 min, 45−15% B; 10−15 min, 15−30% B; 15−30 min, 30−40% B; 30−40 min, 40−50% B; 40−60 min, 50−95% B; 60−70 min, back to 5% B.

Extraction and Isolation of Phenolic Phytochemicals. The air-dried soybean leaves (4.0 kg) collected at growth stage 7 (R7) after seeding were chopped and extracted with EtOAc (12 L) at room temperature for 7 days. The extract was evaporated to dryness under reduced pressure at a temperature below 35 °C to afford EtOAc-soluble extracts (76 g). The EtOAc extract was subjected to column chromatography (CC) on silica gel (10 × 40 cm, 230−400 mesh, 750 g) using a hexane to acetone gradient (50:1→1:1) to give eight fractions (A−H). Fraction C (1.8 g) was fractionated by silica gel flash CC employing a gradient of hexane to acetone, resulting in nine subfractions. Subfractions (C6−C8), enriched with compounds **3** and **8**, were combined (362 mg) and further purified by reversed-phase CC (ODS-A, 12 nm, S-150 μM) eluting with CH_3OH/H_2O (4:1) to afford compounds **3** (42 mg) and **8** (3.2 mg). Fraction D (3.1 g) was fractionated by silica gel flash CC employing a gradient of hexane to acetone, resulting in 25 subfractions. Subfractions (D12−D23), enriched with compounds **9** and **10**, were combined (308 mg) and further purified by Sephadex LH-20 (Pharmacia Biotech AB) with 80% CH_3OH as eluent, yielding compounds **9** (17 mg) and **10** (13 mg). Fraction E (4.6 g) was subjected to flash CC employing a gradient of $CHCl_3$ to EtOAc, giving 12 subfractions. Subfractions E2 and E3 were purified using Sephadex LH-20 column chromatography, eluting with 95% CH_3OH to afford compound **7** (8 mg). Subfractions (E4−E11), enriched with compounds **1**, **2**, and **4**, were combined (461 mg) and further purified by reversed-phase CC (ODS-A, 12 nm, S-150 μM) eluting with CH_3OH/H_2O (3:2) to afford compounds **1** (158 mg), **2** (20 mg), and **4** (22 mg). Fraction F (4.1 g) was subjected to reversed-phase CC (ODS-A, 12 nm, S-150 μM) eluting with CH_3OH/H_2O (4:1) to afford compounds **6** (16 mg) and **5** (14 mg). All isolated compounds were identified on the basis of the following spectroscopic data.

*Coumestrol (**1**):* yellow needles; mp >300 °C; EIMS, m/z 268 $[M]^+$; HREIMS, m/z 268.0373 (calcd for $C_{15}H_8O_5$ 268.0372); ^{1}H NMR (500 MHz, DMSO-d_6) δ 6.91 (1H, d, J = 1.9 Hz, H-4), 6.93 (1H, dd, J = 8.5, 2.1 Hz, H-2), 6.95 (1H, dd, J = 8.3, 2.1 Hz, H-8), 7.17 (1H, d, J = 1.9 Hz, H-10), 7.69 (1H, d, J = 8.4 Hz, H-7), 7.85 (1H, d, J = 8.4 Hz, H-1).

*Isotrifoliol (**2**):* pale-yellow needles; mp >300 °C; EIMS, m/z 298 $[M]^+$; HREIMS, m/z 298.0476 (calcd for $C_{16}H_{10}O_6$ 298.0477); ^{1}H NMR (500 MHz, DMSO-d_6) δ 3.98 (1-OCH_3), 6.51 (1H, s, H-2), 6.52 (1H, s, H-4), 6.94 (1H, d, J = 8.4 Hz, H-8), 7.13 (1H, s, H-10), 7.68 (1H, d, J = 8.4 Hz, H-7).

*Phaseol (**3**):* white needles; mp 248−250 °C; EIMS, m/z 336 $[M]^+$; HREIMS, m/z 336.1004 (calcd for $C_{20}H_{16}O_5$ 336.0998); ^{1}H NMR (500 MHz, DMSO-d_6) δ 1.63 (3H, s, H-5′), 1.82 (3H, s, H-4′), 3.46 (2H, d, J = 7.1 Hz, H-1′), 5.22 (1H, t, J = 7.2, 6.3 Hz, H-2′), 6.94 (1H, d, J = 8.4 Hz, H-8), 6.98 (1H, d, J = 8.6 Hz, H-2), 7.15 (1H, s, H-10), 7.68 (1H, s, H-7), 7.70 (1H, s, H-1).

*Glyceollin I (**4**):* amorphous yellow powder; mp 154−158 °C; EIMS, m/z 338 $[M]^+$; HREIMS, m/z 338.1161 (calcd for $C_{20}H_{18}O_5$

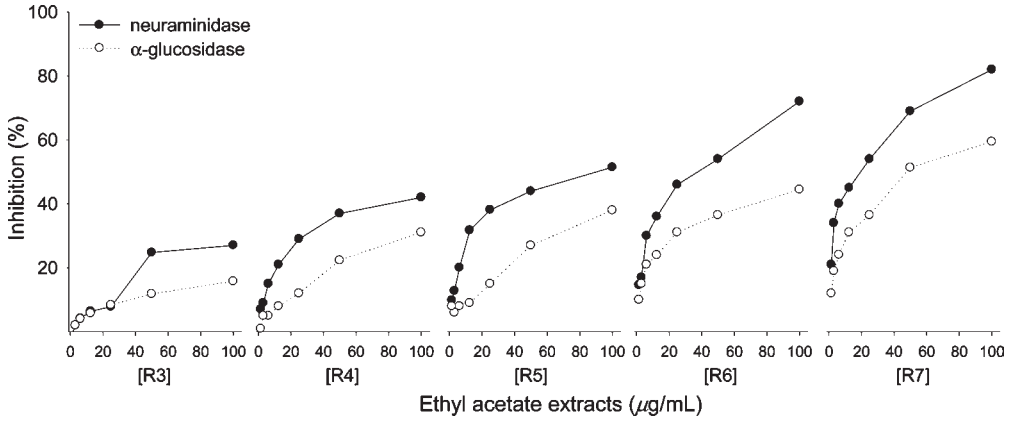

Figure 1. Glycosidase inhibitory activities of ethyl acetate extracts from soybean leaves at different growth stages (R3−R7). Values, reported as inhibition ratio (%), are the mean ± SD of measurements carried out on three independent samples analyzed three times.

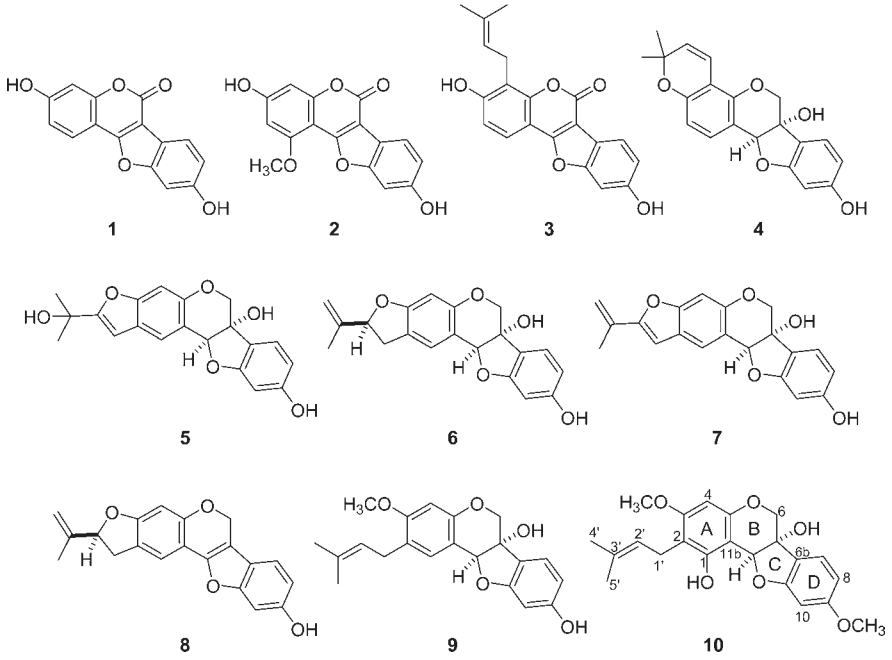

Figure 2. Chemical structures of isolated pterocarpans **1**−**10** from soybean leaves.

338.1154); ^{1}H NMR (500 MHz, CH_3OH) δ 1.39 (3H, s, H-15), 1.40 (3H, s, H-16), 3.92 (1H, d, J = 11.4 Hz, H-6α), 4.13 (1H, d, J = 11.4 Hz, H-6ß), 5.18 (1H, s, H-11a), 5.63 (1H, d, J = 9.8 Hz, H-13), 6.24 (1H, s, H-10), 6.26 (1H, d, J = 8.1 Hz, H-8), 6.40 (1H, d, J = 8.4 Hz, H-2), 6.43 (1H, d, J = 9.8 Hz, H-12), 7.11 (1H, d, J = 8.1 Hz, H-7), 7.17 (1H, d, J = 8.4 Hz, H-1).

Glyceofuran (***5***)*:* colorless needles; mp 181−183 °C; EIMS, m/z 354 $[M]^+$; HREIMS, m/z 354.1127 (calcd for $C_{20}H_{18}O_6$ 354.1103); ^{1}H NMR (500 MHz, CH_3OH) δ 1.62 (6H, s, H-15, 16), 3.98 (1H, d, J = 11.4 Hz, H-6α), 4.18 (1H, d, J = 11.4 Hz, H-6ß), 5.39 (1H, s, H-11a), 6.25 (1H, d, J = 1.9 Hz, H-10), 6.43 (1H, dd, J = 8.2, 2.1 Hz, H-8), 6.62 (1H, d, J = 0.7 Hz, H-12), 6.99 (1H, s, H-4), 7.20 (1H, d, J = 8.2 Hz, H-7), 7.65 (1H, s, H-1).

Glyceollin III (***6***)*:* colorless needles; mp 148−152 °C; EIMS, m/z 338 $[M]^+$; HREIMS, m/z 338.1158 (calcd for $C_{20}H_{18}O_5$ 338.1154); ^{1}H NMR (500 MHz, CD_3OD) δ 1.75 (3H, s, H-16), 3.00 (1H, m, H-12α), 3.37 (1H, m, H-12ß), 3.90 (1H, d, J = 11.3 Hz, H-6α), 4.12 (1H, d, J = 11.3 Hz, H-6ß), 4.89 (1H, m, H-15a), 4.91 (1H, s, H-11a), 5.20 (1H, m, H-15b), 5.21 (1H, t, J = 8.1 Hz, H-13), 6.24 (1H, s, H-10), 6.28 (1H, s, H-4), 6.41 (1H, dd, J = 8.1, 2.1 Hz, H-8), 7.17 (1H, d, J = 8.1 Hz, H-7), 7.25 (1H, s, H-1).

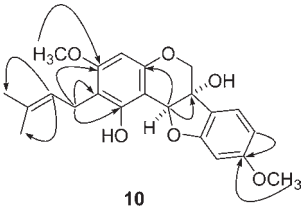

Figure 3. Selected HMBC correlations for new pterocarpan **10**.

Glyceollin VII (***7***)*:* yellowish powder; mp 149−151 °C; $[\alpha]_D^{20}$ −142 (c 0.26, CH_3OH); EIMS, m/z 336 $[M]^+$; HREIMS, m/z 336.1007 (calcd for $C_{20}H_{16}O_5$ 336.0998); CD (DMSO) λ_{max} $\Delta\varepsilon$ nm +166.7 (289),

−57.6 (235); ^{1}H NMR (500 MHz, CD_3OD) δ 2.00 (3H, s, H-16), 3.90 (1H, d, J = 11.4 Hz, H-6α), 4.07 (1H, d, J = 11.4 Hz, H-6ß), 5.04 (1H, s, H-15b), 5.27 (1H, s, H-11a), 5.58 (1H, s, H-15a), 6.14 (1H, s, H-10), 6.31 (1H, dd, J = 8.1, 1.5 Hz, H-8), 6.61 (1H, s, H-12), 6.86 (1H, s, H-4), 7.09 (1H, d, J = 8.1 Hz, H-7), 7.55(1H, s, H-1).

*Glyceollin VI (**8**):* yellow solid; mp 147−150 °C; $[\alpha]_D^{23}$ +42.8 (c 0.24, CH_3OH); EIMS, m/z 320 $[M]^+$; HREIMS, m/z 320.1050 (calcd for $C_{20}H_{16}O_4$ 320.1049); ^{1}H NMR (500 MHz, CD_3OD) δ 1.73 (3H, s, H-16), 2.97 (1H, m, H-12α), 3.33 (1H, m, H-12ß), 4.89 (1H, s, H-15a), 5.06 (1H, s, H-15b), 5.19 (1H, t, J = 8.6 Hz, H-13), 5.45 (1H, s, H-6α), 5.47 (1H, s, H-6ß), 6.34 (1H, s, H-4), 6.74 (1H, dd, J = 8.4, 2.1 Hz H-8), 6.92 (1H, s, H-10), 7.06 (1H, dd, J = 8.4, 2.1 Hz, H-7), 7.23 (1H, s, H-1).

*Glyceollin IV (**9**):* yellowish powder; mp 149−151 °C; EIMS, m/z 354 $[M]^+$; HREIMS, m/z 354.1467 (calcd for $C_{21}H_{22}O_5$ 354.1467); CD (CH_3OH) λ_{max} $\Delta\varepsilon$ nm +61.7 (290), −157.6 (240); ^{1}H NMR (500 MHz, CD_3OD) δ 1.70 (3H, s, H-5′), 1.74 (3H, s, H-4′), 3.23 (2H, m, H-1′), 3.76 (3-OCH_3), 3.90 (1H, d, J = 11.4 Hz, H-6α), 4.10 (1H, d, J = 11.4 Hz, H-6ß), 5.16 (1H, s, H-11a), 5.26 (1H, m, H-2′), 6.23 (1H, s, H-10), 6.39 (1H, d, J = 8.2 Hz, H-8), 6.42 (1H, s, H-4), 7.13 (1H, s, H-1), 7.15 (1H, d, J = 8.2 Hz, H-7).

*Glyceollin VIII (**10**):* yellowish powder; mp 151−154 °C; $[\alpha]_D^{20}$ −162 (c 0.26, CH_3OH); EIMS, m/z 384 $[M]^+$; HREIMS, m/z 384.1572 (calcd for $C_{22}H_{24}O_6$ 384.1573); CD (CH_3OH) λ_{max} $\Delta\varepsilon$ nm +54.3 (295), −156.5 (251); ^{1}H NMR and ^{13}C NMR data, see Table 1.

Table 2. Inhibitory Effects of Compounds 1−10 on Neuraminidase and α-Glucosidase Activities

	neuraminidase		α-glucosidase
compound	IC_{50}[a] (μM)	kinetic mode (K_i[b], μM)	IC_{50} (μM)
1	37.8 ± 0.8	noncompetitive (44.8)	6.0 ± 0.6
2	>100	nt[c]	23.0 ± 1.6
3	>100	nt	42.6 ± 1.9
4	89.4 ± 1.3	nt	>100
5	22.6 ± 0.6	noncompetitive (21.6)	>100
6	3.6 ± 1.6	noncompetitive (3.3)	>100
7	2.4 ± 1.9	noncompetitive (1.9)	90.4 ± 1.9
8	4.0 ± 1.9	noncompetitive (3.7)	>100
9	23.1 ± 0.6	noncompetitive (23.3)	>100
10	32.4 ± 1.4	noncompetitive (35.8)	>100
quercetin	17.4 ± 1.2	nt	nt

[a] All compounds were examined in a set of experiments repeated three times; IC_{50} values of compounds represent the concentration that caused 50% enzyme activity loss. [b] Values of inhibition constant. [c] nt, not tested.

Assay of Glycosidase Activity. Neuraminidase (EC 3.2.1.18. from *Clostridium perfringens*, Sigma-Aldrich, St. Louis, MO), α-glucosidase (EC 3.2.1.20), β-glucosidase (EC 3.2.1.21), α-mannosidase (EC 3.2.1.24), and α-rhamnosidase (EC 3.2.1.40) inhibitory activities were calculated using literature experimental procedures with some modifications. All enzyme activities were determined using the appropriate substrates (4-methylumbelliferyl-α-D-*N*-acetylneuraminic acid, *p*-nitrophenyl-α-D-glucopyranoside, *p*-nitrophenyl-β-D-glucopyranoside, *p*-nitrophenyl-α-D-mannopyranoside, and *p*-nitrophenyl-α-D-rhamnopyranoside, respectively) at the optimum pH of each enzyme. The reaction was stopped by adding 2 M NaOH. Glycosidases were assayed according to standard procedures by following the hydrolysis of 4-methylumbelliferyl-α-D-*N*-acetylneuraminic acid (for neuraminidase) or nitrophenyl glycosides (all others) spectrophotometrically fluorometrically on a

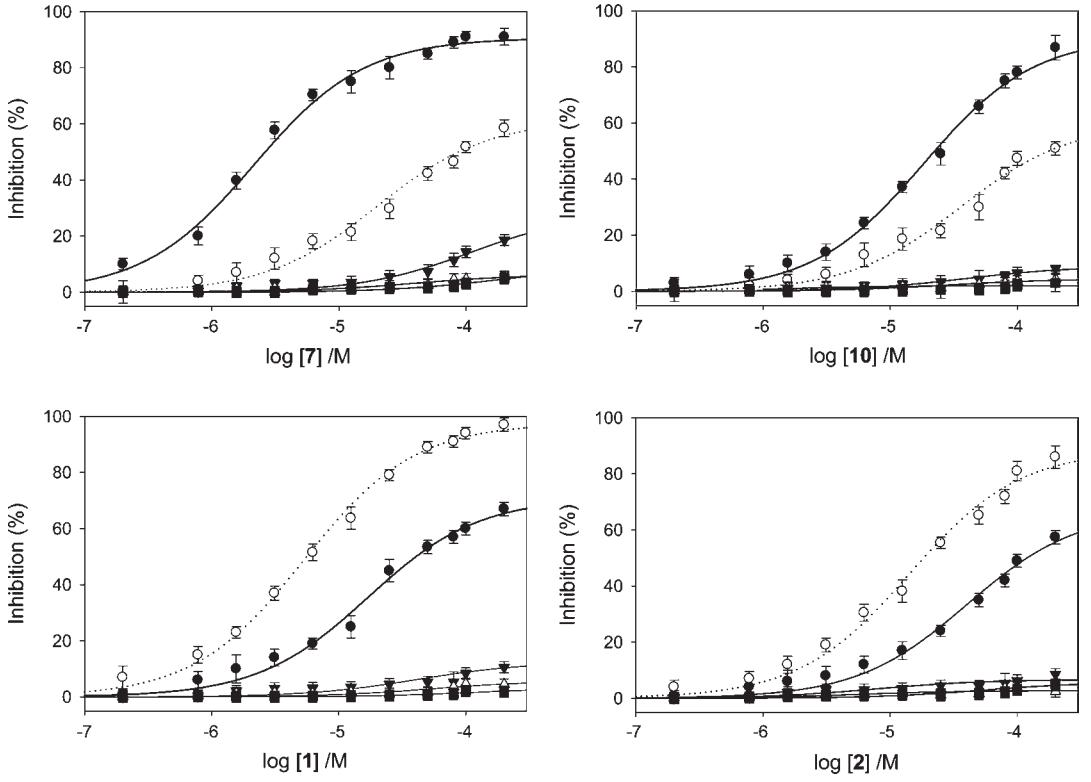

Figure 4. Inhibitory selectivity of 6a-hydroxypterocarpans (**1**, **2**) and coumestanes (**7**, **10**) with related glycosidase. Inhibitors were tested on glycosidases (neuraminidase, ●; α-glucosidase, ○; β-glucosidase, ▼; α-mannosidase, Δ; α-rhamnosidase, ■). Data represent the results of three independent experiments performed with three replicates per sample.

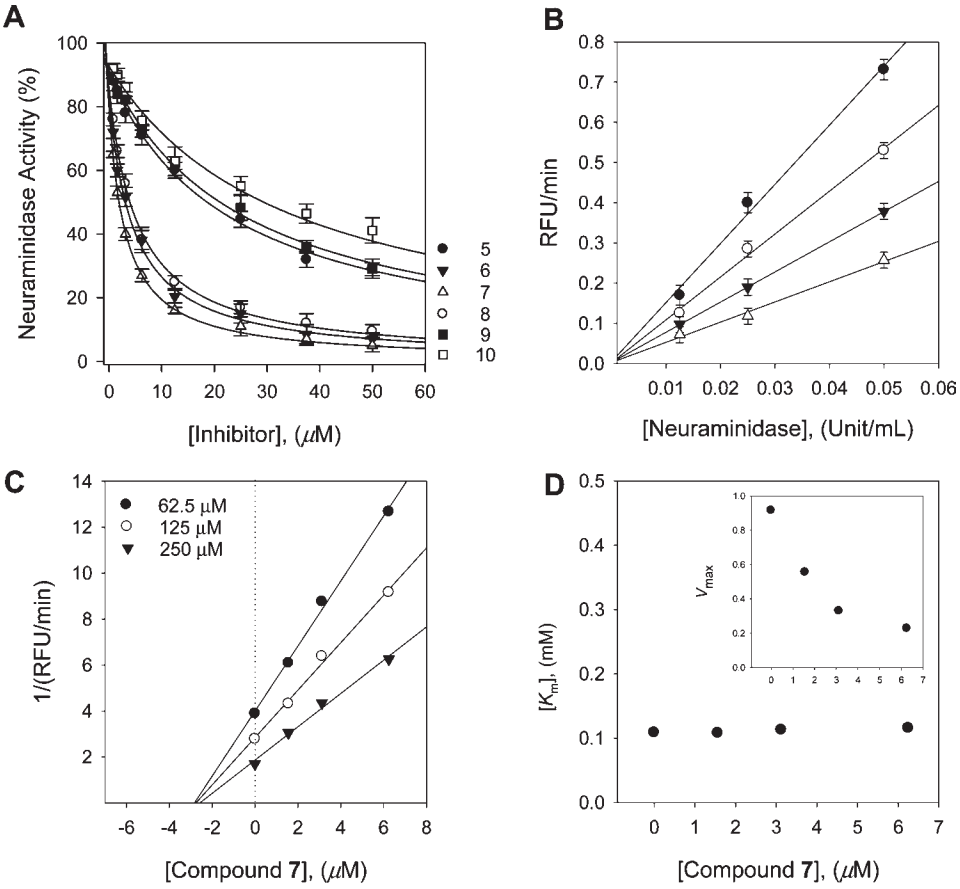

Figure 5. (A) Effects of compounds on the activity of neuraminidase for hydrolysis of 4-methylumbelliferyl-α-D-*N*-acetylneuraminic acid (compound **5**, ●; compound **6**, ▼; compound **7**, Δ; compound **8**, ○; compound **9**, ■; compound **10**, □). (B) Hydrolytic activity of neuraminidase as a function of concentration of compound **7** (0, ●; 1.5 μM, ○; 3.1 μM, ▼; 6.2 μM, Δ). (C) Dixon plots of neuraminidase inhibition by compound **7**. The graphical symbols are substrate concentrations (62.5 μM, ●; 125 μM, ○; 250 μM, ▼). (D) K_m values as a function of the concentrations of compound **7**. (Inset) Dependence of the values of V_{max} on the concentration of compound **7**.

SpectraMax M3Multi-Mode Microplate Reader (Molecular Devices, Sunnyvale, CA).[13−16] The inhibitory effects of the tested compounds were expressed as the concentrations that inhibited 50% of the enzyme activity (IC_{50}). Kinetic parameters were determined using the Lineweaver−Burk double-reciprocal plot and Dixon plot methods at increasing concentrations of substrates and inhibitors. The inhibitors deoxynorijirimycin (Sigma-Aldrich, St. Louis, MO) and quercetin (Sigma-Aldrich) were used in the assays for comparison. All parameters were then calculated using SigmaPlot (Systat Software Inc.).

Statistical Analysis. Statistical analysis was undertaken using the general linear model procedure (GLM) from SAS statistical software Institute (version 9.1, 2002, SAS, Cary, NC). All determinations were based on three replicate samples, and the results for content are shown as mean values. Differences between the means of sample were analyzed by the least significant differences test at a probability level of 0.05.

RESULTS AND DISCUSSION

The study began by collecting soybean leaves sequentially at stages between R1 (beginning flowering) and R7 (beginning maturity) and extracting them into ethyl acetate. The obtained crude ethyl acetate extracts were screened and evaluated initially for their inhibitory properties against a range of glycosidases and subsequently for their pterocarpan contents by HPLC (vide infra). All assessments of glycosidase inhibition were carried out according to standard literature procedures, by following the inhibitory effect of each extract on the respective glycosidase spectrophotometrically. To determine the specificity of each extract with respect to specific glycosidases, the relative inhibitory potencies against the enzymes α-glucosidase, β-glucosidase, α-mannosidase, α-rhamnosidase, and neuraminidase were examined. All extracts exhibited significant and dose-dependent inhibitory effects on α-glucosidase and neuraminidase. However, none of the extracts showed any activity against the other glycosidases at concentrations up to 200 μg/mL. Having identified α-glucosidase and neuraminidase as the only target enzymes from our assay group, we determined the relative effectiveness of the extract of each growth stage by subjecting these enzymes to increasing amounts of ethyl acetate extracts (6.25, 12.5, 25, 50, and 100 μg/mL) (Figure 1). Inhibitory potency of neuraminidase increased as a function of plant maturity: R3 (IC_{50} > 200 μg/mL) < R4 (IC_{50} = 154.5 μg/mL) < R5 (IC_{50} = 93.5 μg/mL) < R6 (IC_{50} = 34.7 μg/mL) < R7 (IC_{50} = 20.4 μg/mL). A similar inhibitory pattern was observed against α-glucosidase: R3 (IC_{50} > 200 μg/mL) < R4 (IC_{50} > 200 μg/mL) < R5 (IC_{50} > 200 μg/mL) < R6 (IC_{50} = 134.7 μg/mL) < R7 (IC_{50} = 70.1 μg/mL). This trend also revealed that the extracts preferentially inhibited neuraminidase over α-glucosidase. The specific compounds responsible for these characteristics were continuously identified.

Ten glycosidase inhibitory pterocarpans (**1**−**10**) were isolated from soybean leaves (Figure 2). Compounds **1**−**9** were

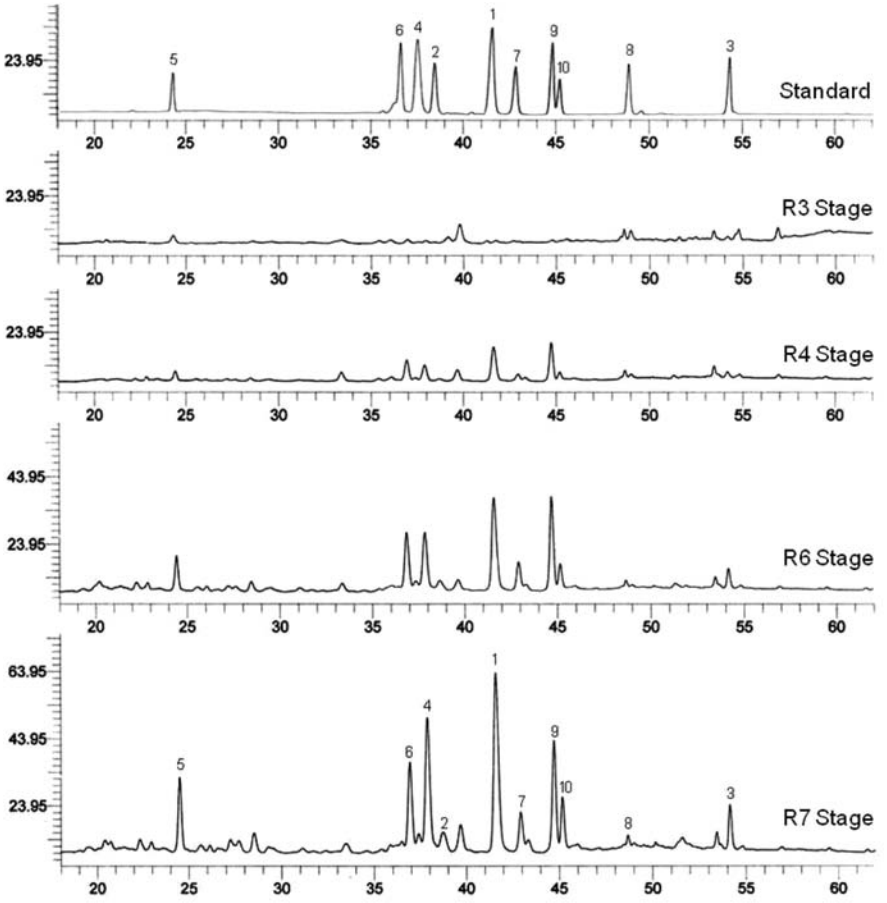

Figure 6. HPLC profiling of pterocarpans at different growth stages (R3, R5, R6, and R7). The HPLC chromatogram was detected at 280 nm UV. Peaks: 1, coumestrol; 2, isotrifoliol; 3, phaseol; 4, glyceollin I; 5, glyceofuran; 6, glyceollin III; 7, glyceollin VII; 8, glyceollin VI; 9, glyceollin IV; 10, glyceollin VIII.

Table 3. Chromatographic and Spectral Characteristics of the Pterocarpans in Soybean Leaves

peak	t_R (min)	λ_{max} (nm)	MS (m/z)	HREIMS	fragments (m/z)	identification
1	41.62	344	268	268.0373	268 (100), 240 (11), 211 (4)	coumestrol
2	38.74	342	298	298.0476	298 (100), 270 (59), 255 (36), 242 (12)	isotrifoliol
3	54.16	344	336	336.1004	336 (54), 319 (42), 280 (100), 268 (32)	phaseol
4	37.91	284	338	338.1161	338 (15), 323 (48), 320 (82), 305 (100)	glyceollin I
5	24.52	286	354	354.1127	354 (25), 339 (100), 336 (36)	glyceofuran
6	36.95	287	338	338.1158	338 (15), 320 (100), 305 (89), 149 (54)	glyceollin III
7	42.96	285	336	336.1007	336 (9), 329 (16), 318 (100), 178 (38)	glyceollin VII
8	48.69	333	320	320.1050	320 (100), 319 (54), 305 (89), 277 (11)	glyceollin VI
9	44.75	286	354	354.1467	336 (100), 335 (83), 321 (9), 277 (11)	glyceollin IV
10	45.20	284	384	384.1572	384 (17), 366 (100), 365 (77), 351 (19)	glyceollin VIII

identified as known compounds coumestrol (**1**), isotrifoliol (**2**), phaseol (**3**), glyceollin I (**4**), glyceofuran (**5**), glyceollin III (**6**), glyceollin VII (**7**), glyceollin VI (**8**), and glyceollin IV (**9**) by comparing our spectroscopic data with those previously reported.[16−20] New compound **10** was obtained as a yellowish powder with the molecular formula $C_{22}H_{24}O_6$ and 11 degrees of unsaturation established by HREIMS (m/z 384.1572 [M^+], calcd 384.1573). ^{1}H and ^{13}C NMR data in conjuncation with a DEPT experiment indicated the presence of 22 carbon atoms, consisting of the following functional groups: 2 methylenes (sp^3), 1 methine (sp^3), 5 methines (sp^2), 4 methyls, and 10 quaternary carbons (Table 1). The ^{13}C NMR data enabled carbons corresponding to 7 C−C double bonds to be identified, and thus accounted for 7 of the 11 degrees of unsaturation. The extra four degrees of unsaturation were ascribed to four rings, two of which were aromatic. According to ^{13}C and ^{1}H NMR spectra, compound **10** was found to contain both an oxygenated sp^3 methylene (diastereotopic protons: Hα δ_H 3.86, d; and Hβ δ_H 4.05, d) and an oxygenated methine (δ_H 5.33, s). The overall NMR characteristics suggested that **10** bears a 6a-hydroxypterocarpan

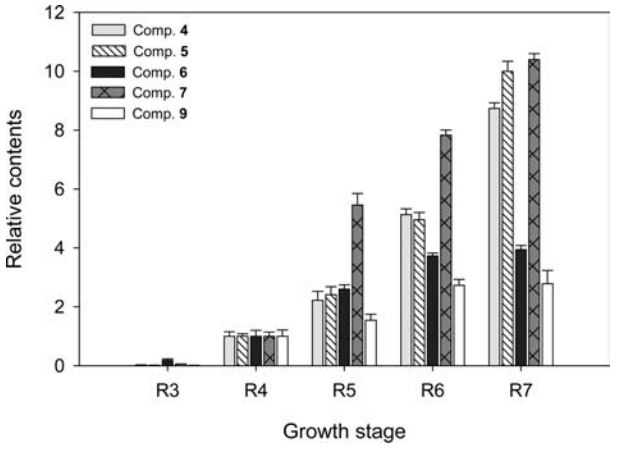

Figure 7. Comparative change of individual 6a-hydroxypterocarpan contents at different growth stages (R3 and R5−R7). Calculation was based on the area of HPLC analysis. Values, reported as relative contents versus the amount of individual pterocarpans at R4 stage, are the mean ± SD of measurements carried out on three independent samples analyzed three times.

backbone.[21] Proton coupling networks (H-1′/H-2′, H-2′/H-4′, and H-5′) in the COSY spectrum revealed a 3,3-dimethylallyl group. HMBC correlation of H-1′ with C-1, C-2, and C-3 revealed that the 3,3-dimethylallyl group was situated on C-2 (Figure 3). The ^{1}H NMR signals of δ_H 3.90 (3H, s) and 3.75 (3H, s) were derived from methoxy groups. The methoxy groups were shown to be positioned at C-3 and C-9 by HMBC correlations between OCH_3/C-3 (δ_C 63.8) and OCH_3/C-9 (δ_C 56.5). The AB aromatic proton spin systems (δ_H 7.15, d, for H-7; δ_H 6.40, d, for H-8) and a single aromatic proton (δ_H 6.25 for H-10) further indicated the presence of a methoxy group on C-9. From HMBC correlations of H-4 with both C-3 (δ_C 161.3) and C-4a (δ_C 156.6), the position of the hydroxyl group was inferred to be at C-1. The absolute configuration at C-6a and C-11a was assigned as *S* from its negative optical rotation ($[\alpha]_D^{20}$ −192, *c* 0.26, CH_3OH), negative Cotton effect of ca. 250 nm, and positive CD peaks at ca. 290 nm.[22] Thus, compound **10** was characterized as (6a*S*,11a*S*)-3,6a-dihydroxy-2-(3,3-dimethylallyl)-1,9-dimethoxypterocarpan and named glyceollin VIII.

Given the data from the crude extracts, all isolated pterocarpans (**1**−**10**) were screened for their inhibition of α-glucosidase and neuraminidase. These compounds showed potent inhibition against α-glucosidase and/or neuraminidase, but they showed no inhibition against other glycosidases studied above (Table 2). The structure of the pterocarpan affected its inhibitory potency significantly. Consistent with the data from the crude leaf extract, the 6a-hydroxypterocarpan series proved to be more effective against neuraminidase (IC_{50} values ranging from 2.4 to 89.4 μM) than against α-glucosidase (IC_{50} ranging from 94.4 μM to >100 μM). Figure 4 describes the inhibitory selectivity of 6a-hydroxypterocarpans (**7**, **10**) and coumestanes (**1**, **2**) with related glycosidases. 6a-Hydroxypterocarpan **7** inhibited neuraminidase with an IC_{50} of 2.4 μM, whereas it inhibited α-glucosidase with an IC_{50} of 90.4 μM. The coumestan series was effective against α-glucosidase, with IC_{50} values ranging from 6.0 to 42.6 μM, which compares favorably to neuraminidase inhibition (IC_{50} > 37.8 μM). These inhibitory features encouraged us to investigate the relationship between 6a-hydroxypterocarpans and neuraminidase. All pterocarpans **5**−**10** exhibited a significant, dose-dependent degree of inhibition (Figure 5A). However, the activity was affected by subtle changes in structure. Ring closure of the prenyl group onto C3-OH to form pentacyclic structures (**6**, **7**, and **8**) gave significant activity, with IC_{50} values of 3.6, 2.4, and 4.0 μM, respectively. However, hydrated pentacycle **5** was less potent (IC_{50} = 22.6 μM). Capping the 6a-hydroxypterocarpan with a methyl group on C3-OCH_3 also gave lower potency (IC_{50} = 23.1 μM). The inhibition of neuraminidase by compound **7** is illustrated in Figure 5B, representatively. Plots of initial velocity versus enzyme concentration in the presence of different concentrations of compound **7** gave a family of straight lines, all of which passed through the origin. Increasing the inhibitor concentration lowered the line gradients, indicating that the compound was a reversible inhibitor. The Dixon plot of **7** versus $1/V$ resulted in a family of straight lines with a common *x*-axis intercept (Figure 5C). Furthermore, the V_{max} decreased while K_m remained constant with increasing concentrations of inhibitor **7** (Figure 5D). These indicate that pterocarpan **7** exhibits noncompetitive inhibition of neuraminidase.

To set the importance of isolated pterocarpans in a practical content, a comprehensive profile of the constituents of the ethyl acetate extract of soybean leaves as a function of growth stage was established as shown in Figure 6. The compounds represented by the 10 main pterocarpans peaks (**1**−**10**) were collected and identified. The nature of each peak in the HPLC trace was doubly verified by comparison with retention time of the pure compound and also by LC-MS (Figure 6 and Table 3). All compounds examined in this study were detected in the HPLC chromatogram such as 41.6 min, coumestrol (**1**); 38.7 min, isotrifoliol (**2**); 54.1 min, phaseol (**3**); 37.9 min, glyceollin I (**4**); 24.5 min, glyceofuran (**5**); 36.9 min, glyceollin III (**6**); 42.9 min, glyceollin VII (**7**); 48.7 min, glyceollin VI (**8**); 44.7 min, glyceollin IV (**9**); and 45.2 min, glyceollin VIII (**10**). We chose to measure absorbance at 280 nm because this was closer to the λ_{max} of the pterocarpans (**1**−**10**). In fact, 6a-hydroxypterocarpans were not detected properly at 254 nm, where the focus of earlier publications, the coumestol series, absorbed.[20] Levels of individual pterocarpans in leaves increased dramatically from the R3 to R7 stage. Most pterocarpans appeared at the R3 stage, and a rapid increase in pterocarpan concentration was observed onward to R7. To measure the relative change of the 6a-hydroxypterocarpans in different growth stages, HPLC analysis was used. The areas of each pterocarpan peak were quantified relative to each peak at the R4 growth stage as shown Figure 7. A correlation between advance in growth stage and concentration of pterocarpan is apparent. The most rapid change was observed in compounds **5** and **7**, both of which increased almost 10-fold between R4 and R7.

In conclusion, the soybean leaves were found to be a rich source of pterocarpan-derived neuraminidase and α-glucosidase inhibitors. The principal components were pterocarpans, of which **10** was defined as a novel compound named glyceollin VIII. The relationship between structure and enzyme inhibition was investigated: 6a-hydroxypterocarpans exhibited much higher inhibition against neuraminidase than against α-glucosidase, whereas coumestrol showed the reverse trend. We proceeded to carry out a quantitative analysis of the onset and changes in concentrations of these 6a-hydroxypterocarpans as a function of growth stage of the plant from R3 to R7. The emergence and peak of 6a-hydroxypterocarpans coincided with the onset and increase in potency of neuraminidase inhibition in the crude extract of the plant.

AUTHOR INFORMATION

Corresponding Author

*Phone: +82-55-772-1965. Fax: +82-55-772-1969. E-mail: khpark@gnu.ac.kr.

Funding Sources

This work was supported by a grant from the Next-Generation BioGreen 21 program (SSAC, No. PJ008107), Rural Development Administration, Republic of Korea. H.J.Y. was supported by a scholarship from the BK21 program.

ABBREVIATIONS USED

IC_{50}, inhibitor concentration leading to 50% activity loss; K_i, inhibition constant; K_m, Michaelis−Menten constant.

REFERENCES

(1) Shental-Bechor, D.; Levy, Y. Effect of glycosylation on protein folding: a close look at thermodynamic stabilization. *Proc. Natl. Acad. Sci. U.S.A.* **2008**, *105*, 8256–8261.

(2) Zhao, H.; Sun, L.; Wang, L.; Xu, Z.; Zhou, F.; Su, J.; Jin, J.; Yang, Y.; Hu, Y.; Zha, X. *N*-glycosylation at Asn residues 554 and 566 of E-cadherin affects cell cycle progression through extracellular signal-regulated protein kinase signaling pathway. *Acta Biochim. Biophys. Sin.* **2008**, *40*, 140–148.

(3) Asano, N. Glycosidase inhibitors: update and perspectives on practical use. *Glycobiology* **2003**, *13*, 93R–104R.

(4) Jacob, G. S. Glycosylation inhibitors in biology and medicine. *Curr. Opin. Struct. Biol.* **1995**, *5*, 605–611.

(5) Du, J.; Meledeo, M. A.; Wang, Z.; Khanna, H. S.; Paruchuri, V. D. P.; Yarema, K. J. Metabolic glycoengineering: Sialic acid and beyond. *Glycobiology* **2009**, *19*, 1382–1401.

(6) Meo, C. D.; Priyadarshani, U. C-5 Modifications in *N*-acetyl-neuraminic acid: scope and limitations. *Carbohydr. Res.* **2008**, *343*, 1540–1552.

(7) Paulson, J. C.; Kawasaki, N. Sialidase inhibitors DAMPen sepsis. *Nat. Biotechnol.* **2011**, *29*, 406–407.

(8) Clercq, E. D. The next ten stories on antiviral drug discovery (part E): advents, advances, and adventures. *Med. Res. Rev.* **2010**, *31*, 118–160.

(9) Nguyen, P. H.; Nguyen, T. N. A.; Kang, K. W.; Ndinteh, D. T.; Mbafor, J. T.; Kim, Y. R.; Oh, W. K. Prenylated pterocarpans as bacterial neuraminidase inhibitors. *Bioorg. Med. Chem.* **2010**, *18*, 3335–3344.

(10) Kim, H. J.; Suh, H. J.; Lee, C. H.; Kim, J. H.; Kang, S. C.; Park, S.; Kim, J. S. Antifungal activity of glyceollins isolated from soybean elicited with *Aspergillus sojae*. *J. Agric. Food Chem.* **2010**, *58*, 9483–9487.

(11) Kim, H. J.; Suh, H. J.; Kim, J. H.; Park, S.; Joo, Y. C.; Kim, J. S. Antioxidant activity of glyceollins derived from soybean elicited with *Aspergillus sojae*. *J. Agric. Food Chem.* **2010**, *58*, 11633–11638.

(12) Payton-Stewart, F.; Khupse, R. S.; Boue, S. M.; Elliott, S.; Zimmermann, M. C.; Skripnikova, E. V.; Ashe, H.; Tilghman, S. L.; Beckman, B. S.; Cleveland, T. E.; McLachlan, J. A.; Bhatnagar, D.; Wiese, T. E.; Erhardt, P.; Burow, M. E. Glyceollin I enantiomers distinctly regulate ER-mediated gene expression. *Steroids* **2010**, *75*, 870–878.

(13) Ryu, H. W.; Curtis-Long, M. J.; Jung, S.; Jin, Y. M.; Cho, J. K.; Ryu, Y. B.; Lee, W. S.; Park, K. H. Xanthones with neuraminidase inhibitory activity from the seedcases of *Garcinia mangostana*. *Bioorg. Med. Chem.* **2010**, *18*, 6258–6264.

(14) Ryu, H. W.; Lee, B. W.; Curtis-Long, M. J.; Jung, S. I.; Ryu, Y. B.; Lee, W. S.; Park, K. H. Polyphenols from *Broussonetia papyrifera* displaying potent α-glucosidase inhibition. *J. Agric. Food Chem.* **2010**, *58*, 202–208.

(15) Chuankhayan, P.; Rimlumduan, T.; Svasti, J.; Cairns, J. R. K. Hydrolysis of soybean isoflavonoid glycosides by *Dalbergia* β-glucosidases. *J. Agric. Food Chem.* **2007**, *55*, 2407–2412.

(16) Yuk, H. J.; Lee, J. H.; Curtis-Long, M. J.; Lee, J. W.; Kim, Y. S.; Ryu, H. W.; Park, C. G.; Jeong, T. S.; Park, K. H. The most abundant polyphenol of soy leaves, coumestrol, displays potent α-glucosidase inhibitory activity. *Food Chem.* **2011**, *126*, 1057–1063.

(17) Lee, J. H.; Lee, B. W.; Kim, J. H.; Jeong, T. S.; Kim, M. J.; Lee, W. S.; Park, K. H. LDL-antioxidant pterocarpans from roots of *Glycine max* (L.) Merr. *J. Agric. Food Chem.* **2006**, *54*, 2057–2063.

(18) Zhou, Y. Y.; Luo, S. H.; Yi, T. S.; Li, C. H.; Luo, Q.; Hua, J.; Liu, Y.; Li, S. H. Secondary metabolites from *Glycine soja* and their growth inhibitory effect against *Spodoptera litura*. *J. Agric. Food Chem.* **2011**, *59*, 6004–6010.

(19) Abe, N.; Sato, H.; Sakamura, S. Antifungal stress compounds from adzuki bean, *Vigna angularis*, treated with *Cephalosporium gregatum*. *Agric. Biol. Chem.* **1987**, *51*, 349–353.

(20) Lyne, R. L.; Mulheirn, L. J. Minor pterocarpinoids of soybean. *Tetrahedron Lett.* **1978**, *34*, 3127–3128.

(21) Garcez, W. S.; Martins, D.; Garcez, F. R.; Marques, M. R.; Pereira, A. A.; Oliveira, L. A.; Rondon, J. N.; Peruca, A. D. Effect of spores of saprophytic fungi on phytoalexin accumulation in seeds of frog-eye leaf spot and stem canker-resistant and -susceptible soybean (*Glycine max* L.) cultivars. *J. Agric. Food Chem.* **2000**, *48*, 3662–3665.

(22) Li, W.; Koike, K.; Asada, Y.; Hirotani, M.; Rui, H.; Yoshikawa, T.; Nikaido, T. Flavonoids from *Glycyrrhiza pallidiflora* hairy root cultures. *Phytochemistry* **2002**, *60*, 351–355.